HOKKAIDO UNIVERSITY

Title	Spatial distributions of desorbing products in steady-state NO and N2O reductions on Pd(110)
Author(s)	Ma, Yunsheng; Matsushima, Tatsuo; Shobatake, Kosuke et al.
Citation	The Journal of Chemical Physics, 124(14), 144711 https://doi.org/10.1063/1.2189855
Issue Date	2006-04-14
Doc URL	https://hdl.handle.net/2115/8410
Rights	Copyright © 2006 American Institute of Physics.
Type	journal article
File Information	JCP_124_144711.pdf

Hokkaido University Collection of Scholarly and Academic Papers : HUSCAP

Spatial distributions of desorbing products in steady-state NO and N_2O reductions on Pd(110)

Yunsheng Ma and Tatsuo Matsushima[a)]
Catalysis Research Center, Hokkaido University, Sapporo 001-0021 Japan

Kosuke Shobatake
Toyota Physical & Chemical Research Institute, Nagakute, Aichi 480-1192 Japan

Anton Kokalj
Jožef Stefan Institute, 1000 Ljubljana, Slovenia

(Received 21 November 2005; accepted 28 February 2006; published online 14 April 2006)

The angular and velocity distributions of desorbing product N_2 were examined over the crystal azimuth in steady-state NO+CO and N_2O+CO reactions on Pd(110) by cross-correlation time-of-flight techniques. At surface temperatures below 600 K, N_2 desorption in both reactions splits into two directional lobes collimated along 41°–45° from the surface normal toward the [001] and [00$\bar{1}$] directions. Above 600 K, the normally directed N_2 desorption is enhanced in the NO reduction. Each product desorption component, as well as CO_2, shows a fairly asymmetric distribution about its collimation axis. Two factors, i.e., the anisotropic site structures and the reactant orientation and movements, are operative to induce such asymmetry, depending on the product emission mechanism. © *2006 American Institute of Physics*. [DOI: 10.1063/1.2189855]

I. INTRODUCTION

The NO and N_2O reduction by CO and H_2 on palladium and rhodium surfaces has received much attention because of its importance in controlling automobile exhaust gas composition and the peculiar N_2 emission.[1,2] N_2O is not only an undesirable by-product in the catalytic NO reduction but also the key intermediate in controlling the selectivity to N_2.[3,4] Its decomposition largely shares the N_2 emission; however, knowledge of this emission process is still limited. The ordinary kinetic approach is not informative for this process because of the presence of several rapid surface-nitrogen removal pathways after the slow NO dissociation.[5] This paper delivers the first extensive analysis of the angular distributions of desorbing N_2 as well as CO_2 in steady-state NO +CO and N_2O+CO reactions on Pd(110) over the whole crystal azimuth. Similarities and remarkable differences in the angular distributions have been observed for these two reactions, characterizing the surface-nitrogen removal processes. The N_2 and CO_2 desorption shows a fairly asymmetric distribution about their collimation axes.

The desorption dynamics (the spatial, velocity, and internal energy distributions) of reaction products with hyperthermal energy must be sensitive to the structure of reaction sites on which the molecules are formed.[6] The relationship of the desorption dynamics to the site structure should provide the most direct site-identification method applicable in the course of a catalyzed reaction.[4,6] The crystal azimuth dependence of the product distributions has been extensively studied only for the reactive CO_2 desorption on Pd(110) and Pt(110) surfaces.[4] These data have provided the fundamental basis for understanding the relationship between the collimated product desorption and reaction-site structures. Such a relationship can be extended to the orientation of intermediate molecules emitting products directly, i.e., in N_2O decomposition. The detailed distribution analysis of desorbing fragment N_2 will provide information on the movement of parent N_2O as well as its orientation as observed in electron (or photon)-stimulated desorption ion angular distribution (ESDIAD).[7,8]

The inclined N_2 desorption in N_2O decomposition on Pd(110) is useful to analyze the removal pathways of surface nitrogen because the concomitant associative desorption of N(a) emits N_2 sharply along the surface normal and other desorbing products N_2O and NH_3 show a cosine distribution.[2,4,9,10] Measurements of the angular and velocity distributions will provide information on the reaction pathways whenever any step becomes rate determining because these distributions do not involve the reaction rate and are always controlled by their own desorption steps.[4] The distributions of desorbing products in the NO reduction have been analyzed with several relaxation methods, such as modulated molecular beams,[11] angle-resolved (AR) temperature-programmed desorption (TPD), or AR-pressure jumps.[10,12,13] Steady-state conditions, however, could not be established for the reaction, and then both detailed kinetic and dynamic analyses of product desorption processes were seriously limited. In their AR-TPD work of NO on Pd(110) in the presence of CO, Ikai and Tanaka found that the N_2 peak at 490 K involves desorption collimated at 38° off normal toward the [001] direction and desorbing N_2, in the other peak at around 600 K, is collimated at the surface normal.[10] The series of their studies has opened a new approach to surface-nitrogen removal, however, these authors argued that the inclined N_2

[a)]Author to whom correspondence should be addressed. Fax: +81-11-706-9120. Electronic mail: tatmatsu@cat.hokudai.ac.jp

 © 2006 American Institute of Physics

Downloaded 16 Apr 2006 to 133.87.245.210. Redistribution subject to AIP license or copyright, see http://jcp.aip.org/jcp/copyright.jsp

desorption was not involved in a catalytic cycle and assigned it as a stoichiometric reaction mediated by NO desorption.[14] Later, we showed that this inclined N_2 desorption is well reproduced in N_2O decomposition on Pd(110), Rh(110), and Ir(110) as well as in steady-state NO+CO (or H_2) and N_2O+CO (or H_2) reactions on Pd(110).[13,15–22] Thus, the intermediate N_2O(a) formed from the NO(a)+N(a) fast reaction[23–25] has been proposed to be oriented along the [001] direction before dissociation in the course of the catalyzed NO reduction. In the present work, AR-product desorption measurements have been successfully performed at different crystal azimuths for the steady-state NO (or N_2O) +CO reaction and the resultant spatial distributions of all products have been constructed in a three-dimensional way.

Many studies on the collimated fragment desorption from surface molecules have been reported in ESDIAD.[7,8] Fast-desorbing fragments are collimated along the ruptured bond axis, yielding structural information on the adsorbed parent molecules. In the thermal decomposition of adsorbed molecules, however, the released fragment has been believed to be quickly thermalized to the surface temperature before emission because these species interact with attractive forces due to their chemical or physical adsorption potential and the energy relaxation is very fast on metal surfaces.[26] In fact, collimated product desorption in thermal surface reactions has been limited to some associative processes such as $CH_3(a)+H(a)\rightarrow CH_4(g)$ and $CO(a)+O(a)\rightarrow CO_2(g)$.[4] In these cases, significant repulsive forces are exerted from the surface toward the nascent products. Thus, the inclined N_2 emission in N_2O decomposition on Pd(110), Rh(110), and Ir(110) is the first example to show collimated fragment desorption in *thermal decompositions* on solid surfaces.[15–18] Its desorption dynamics will be informative regarding the energy partitioning in the dissociation event. The product N_2 effectively receives repulsive forces along the N_2O molecular axis since recent density-functional theory (DFT) calculations with generalized gradient approximations[27,28] (GGA) and scanning tunneling microscope (STM) and near-edge x-ray-absorption fine structure (NEXAFS) work have confirmed the presence of [001]-oriented N_2O on Pd(110).[29,30] Sharp fragment desorption was once reported in a thermal hydrazine decomposition on Ir(111).[31] The product N_2 desorption around 290 K was sharply collimated along the surface normal in AR-TPD procedures after N_2H_4 exposures at 260 K. However, the reliability of the AR signal is not clear because angle-resolved signals become very poor in thermal desorption work unless the apparatus has at least two slits and a very large pumping speed in either a collimator or a reaction chamber.[32]

II. EXPERIMENT

The apparatus used has three separately pumped chambers.[21] The reaction chamber is equipped with x-ray photoelectron spectroscopy (XPS) optics, reverse-view low-energy electron diffraction (LEED), an ion gun, and a quadrupole mass spectrometer (QMS) for angle-integrated (AI) measurements. The chopper house has a large pumping rate of about 7 $m^3\ s^{-1}$. This high pumping rate can satisfactorily yield angle-resolved measurements.[32] The chopper house has a narrow slit facing the reaction chamber and a cross-correlation random chopper blade. Another QMS was set in the analyzer connected through a narrow tube-type slit for AR-product desorption and time-of-flight (TOF) analyses. The distance from the ionizer to the chopper blade was 377 mm and the time resolution was selected at 20 μs.[33]

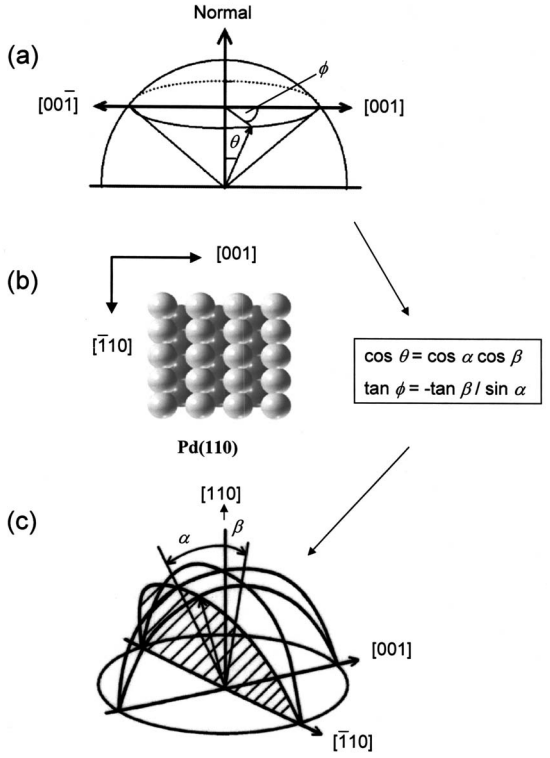

FIG. 1. Definition of the desorption angles and crystal azimuths. (a) The crystal azimuth (ϕ) and desorption angle (θ) used in the experiments. (b) A top view of Pd(110) and the relation of the two angle systems according to the rotation of Eulerian angles (see the text). (c) The new angle system (α,β) in the data analyses. The plane at a fixed α value is shown as crosshatched.

A palladium crystal with a (110) plane (Surface Preparation Laboratory, Netherlands) in a disk-shaped slice (with 1 mm thickness and a 10 mm diameter) was mounted on top of a rotatable manipulator. The crystal was rotated to change the desorption angle (polar angle, θ) in the normally directed plane at various crystal azimuths between the [001] and [$\bar{1}$10] directions. The crystal azimuth (ϕ) is defined in the (110) plane as the angle rotated from the [001] direction, i.e., ϕ=0° at the [001] direction [Fig. 1(a)]. The LEED pattern showed a sharp (1×1) form after the surface was cleaned by Ar^+ ion bombardments in the surface temperature (T_S) range between 800 and 900 K, heating in 5×10^{-8} Torr oxygen at 850 K, and annealing at 1100 K.

$^{15}N_2O$ was introduced through a doser with a small orifice (diameter: 0.1 mm) about 2 cm from the sample crystal, while ^{13}CO and ^{15}NO were backfilled. The partial pressures of $^{13}C^{16}O(P_{CO})$ and $^{15}NO(P_{NO})$ were kept constant by continuously dosing the gas. Hereafter, the isotopes ^{15}N and ^{13}C are, respectively, denoted by N and C in the text. The product N_2, CO_2, and N_2O signals were monitored in both AI and AR forms. The N_2 signals in both QMS's were corrected for

Downloaded 16 Apr 2006 to 133.87.245.210. Redistribution subject to AIP license or copyright, see http://jcp.aip.org/jcp/copyright.jsp

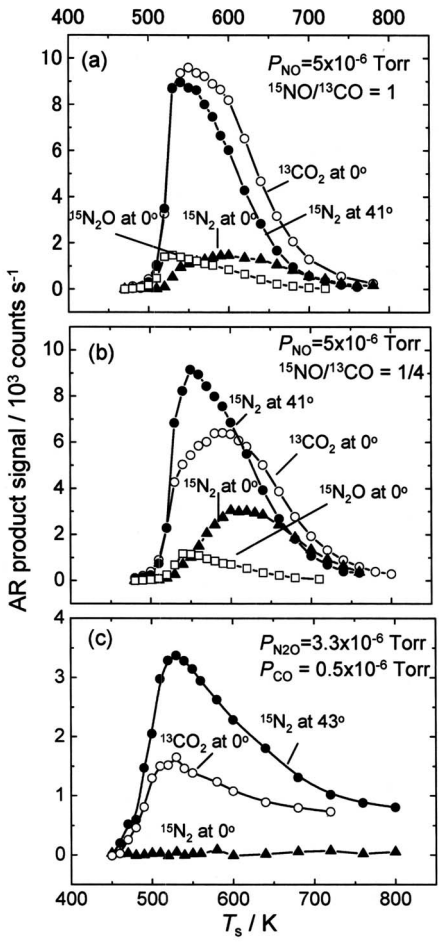

FIG. 2. AR-product signals at the collimation angles in a steady-state [(a) and (b)] NO+CO and (c) N_2O+CO reaction as a function of surface temperature (T_S). In (a) and (b), the P_{NO}/P_{CO} ratio is unity and 1/4, respectively. Open circles: $^{13}CO_2$ at $\theta=0°$; closed circles: $^{15}N_2$ at $\theta=41°$ (or 43° for the $^{15}N_2O$ reduction); closed triangles: $^{15}N_2$ at $\theta=0°$; and open squares: $^{15}N_2O$ at $\theta=0°$.

the contribution of the fragmentation of N_2O. The pressures of reactant gases were also corrected by their mass spectrometer sensitivities.

III. RESULTS

A. General features

The AR signal was obtained with the analyzer QMS as the difference between the signal at the desired angle and the signal when the crystal was away from the line-of-sight position. The above gas doser with a small orifice was effective to reduce the N_2 formation in the N_2O exposure on the reaction chamber wall. Under this construction, the flux of incident N_2O toward the surface decreased proportionally to $\cos(\theta)$ when the angle shifted from the normal direction. This decrement was evaluated and the signal intensity was corrected.[21]

For the steady-state NO+CO reaction at different P_{NO}/P_{CO} ratios, Figs. 2(a) and 2(b) shows the AR signals at around the collimation angles (the maximum flux position) against T_S, at $\theta=0°$ for desorbing N_2, CO_2, and N_2O, and at $\theta=41°$ for the N_2 in the plane along the [001] direction. All the signals were negligible below 490 K. The N_2 signal at $\theta=41°$ increased rapidly above 500 K, reached a maximum at around 550 K, and then decreased at higher temperatures. This signal is due to the inclined N_2 desorption in the intermediate N_2O decomposition.[2,4] The N_2 signal at $\theta=0°$, on the other hand, increased slowly and peaked at about 600 K. This comes from the associative desorption of N(a).[9,10] The AR CO_2 signal at the normal direction increased at around 500 K and decreased above 570 K with increasing T_S, more slowly than the N_2 signal at $\theta=41°$. The temperature dependence of the N_2O signal was very similar to that of N_2 at $\theta=41°$. It should be noted that the ratio of the N_2 signal at 41° to that at 0° decreases with increasing T_S, indicating that the reaction pathway shifts at high temperatures. Nevertheless, the reaction stoichiometry was already confirmed as $xNO+CO \rightarrow yN_2+zN_2O+CO_2$ where $2x=y+z$.[21]

At the pressure ratio of $P_{NO}/P_{CO}=1$, the N_2 signal at $\theta=0°$ was much less than that at 41° below 550 K, i.e., the product N_2 mostly comes from the intermediate N_2O dissociation. Above 650 K, the normally directed N_2 signal overcomes the other. At high temperatures, the amount of NO(a) is reduced, and the N_2O formation is suppressed, whereas the association of N(a) is enhanced because of the higher activation energy.[34] This situation became clear when the CO pressure was increased at the location in which the amount of N(a) was increased by the fast removal of O(a) and the resultant enhanced NO dissociation [Fig. 2(b)].[20] At higher CO pressures, the N_2 signal at $\theta=0°$ was highly enhanced and the N_2 formation shifted from the N_2O decomposition pathway to the association of N(a). Thus, N_2 desorption in the two pathways was examined at both $P_{NO}/P_{CO}=1$ ($T_S=550$ K) and 1/4 ($T_S=640$ K) in this work.

The AR N_2 signal in the N_2O+CO reaction was measurable because of the sharply collimated desorption although the AI N_2 signal involved large experimental uncertainty. The maximum N_2 flux was located at $\theta=43°-46°$ in the N_2O+CO reaction. The signals at their collimation angles at 3.3×10^{-6} Torr of N_2O and 0.5×10^{-6} Torr of CO are plotted versus the surface temperature [Fig. 2(c)]. The AR N_2 signal became noticeable above around 450 K. The signal was peaked at 510 K and decreased quickly at higher temperatures. No AR N_2 signal was found in the normal direction. The desorption of the other product CO_2 collimated along the surface normal. The difference in the signal between N_2 and CO_2 was mostly due to different angular distributions.

In the range of $T_S=400-800$ K, only the (1×1) pattern was observed in LEED measurements during the steady-state CO+NO reaction at a total pressure of 1×10^{-7} Torr of the equimolar mixture of NO and CO. This indicates reducing surface conditions at $P_{NO}/P_{CO}=1$.[20] On the other hand, under a constant N_2O flow at T_S below 350 K, a streaky c(2 $\times$4) structure was observed. Increasing T_S to 470 K resulted in the appearance of (2×3)-1D superstructure spots. They are due to oxygen adsorption.[35] LEED structures were also examined around the kinetic transition under steady-state conditions at different CO pressures.[36] With increasing CO pressure, the intensity of the fractional spot became weaker. When the N_2O/CO pressure ratio was about 13 at the kinetic

Downloaded 16 Apr 2006 to 133.87.245.210. Redistribution subject to AIP license or copyright, see http://jcp.aip.org/jcp/copyright.jsp

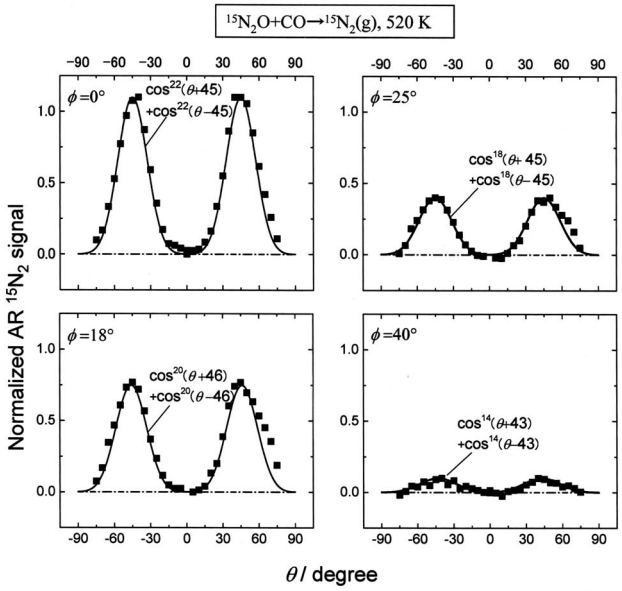

FIG. 3. Angular distributions of desorbing N_2 at different crystal azimuths (ϕ=0°, 18°, 25°, and 40°) in the steady-state N_2O reduction at $P_{N2O}=3.3\times10^{-6}$ Torr, $P_{CO}=0.5\times10^{-6}$ Torr, and T_S=520 K. The signal is normalized to the maximum value at the collimation angle. The solid curves are simulated by the inserted equations.

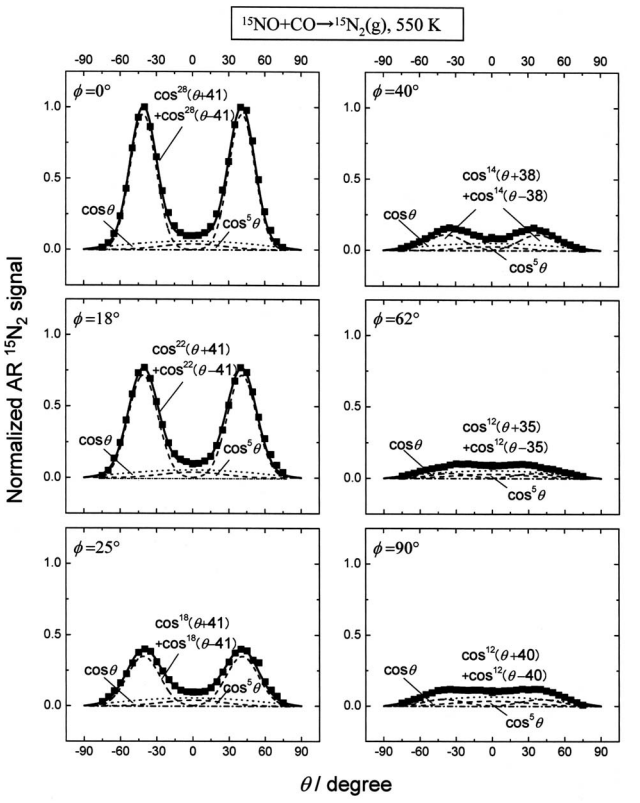

FIG. 4. Angular distributions of desorbing N_2 at different crystal azimuths (ϕ=0°, 18°, 25°, 40°, 62°, and 90°) in the steady-state NO reduction at $P_{NO}=P_{CO}=5\times10^{-6}$ Torr and T_S=550 K. The signal is normalized to the maximum value at the collimation position. Typical deconvolutions are shown by broken and dotted curves. The solid curve indicates the sum of the components.

transition or above it, the pattern was converted from a (1 $\times$1) structure to (2$\times$3)-O lattice. Both N_2O and NO reductions are seriously retarded by adsorbed oxygen,[17,36] and thus the rate-limiting steps of the reactions are likely to proceed on clean parts free from oxygen.

B. Angular distribution and crystal azimuth

In the N_2O+CO reaction desorbing N_2 always split in a two-directional way in the plane along the [001] direction and collimated at θ=43°–46° off the surface normal in the temperature range studied, 460–800 K. No normally directed desorption was found even at 800 K. The distribution became somewhat broader from a $\cos^{28}(45-\theta)$ form at 460 K to a $\cos^{18}(45-\theta)$ form at 750 K, but the collimation angle remained invariant. The angular distributions at different crystal azimuths at 520 K, $P_{N2O}=3.3\times10^{-6}$ Torr and $P_{CO}=0.5\times10^{-6}$ Torr, are shown in Fig. 3. The surface was under the reducing condition because the CO pressure was above the kinetic critical point (P_{N2O}/P_{CO}=13 at 520 K), i.e., CO(a)$\gg$O(a).[36] The observed maximum flux position remains fairly invariant when the crystal azimuth is shifted from the [001] direction. The signal at ϕ=0° (along the [001] direction) is approximated by a $\{\cos^{22}(\theta+45)+\cos^{22}(\theta-45)\}$ form. The distribution becomes broader with an increasing azimuth. The signal intensity itself decreases quickly and is almost completely suppressed above ϕ=40°. The distributions mostly remain invariant even when the CO pressure is lower than the kinetic critical value.

On the other hand, the desorbing N_2 in the NO+CO reaction showed different behavior above 550 K. Below 550 K, the angular distribution of N_2 was quite close to that in the N_2O+CO reaction, indicating a common N_2 emission process. The distributions at 550 K and $P_{NO}=P_{CO}=5\times10^{-6}$ Torr are shown in Fig. 4. This is the optimum condition for N_2 formation from an equimolar (NO+CO) mixture. The signal at ϕ=0° was well approximated by a form of $0.91\{\cos^{28}(\theta+41)+\cos^{28}(\theta-41)\}+0.03\cos^5(\theta)+0.06\cos(\theta)$. The latter two components were estimated from the velocity distribution analysis to be described in the next section. The intensity of these components in the normal direction is independent of the ϕ position. The distribution again becomes broader with increasing azimuth. The signal intensity itself decreases quickly and is mostly suppressed at around ϕ=40°. The remaining signal above ϕ=60° is mostly due to the normally directed and cosine components.

At temperatures above 550 K and smaller P_{NO}/P_{CO} ratios, the distributions change significantly. The typical results are shown for T_S=640 K and a ratio of P_{NO}/P_{CO}=1/4 in Fig. 5. The angular distribution at 640 K involved three desorption components. The normally directed and cosine components are drastically enhanced. The distribution at ϕ=0° is approximated by $0.7\{\cos^{28}(\theta+41)+\cos^{28}(\theta-41)\}+0.25\cos^7(\theta)+0.4\cos(\theta)$ on the basis of the velocity distribution analysis to be described in the following section. The intensity of the latter two components remains invariant. Only the intensity of the inclined component decreases with increasing azimuth. The cosine component predominates at crystal azimuths above ϕ=25°.

The CO_2 desorption collimates sharply along the surface normal in both N_2O and NO reduction. No differences have been found in the CO_2 distribution between them. The results

Downloaded 16 Apr 2006 to 133.87.245.210. Redistribution subject to AIP license or copyright, see http://jcp.aip.org/jcp/copyright.jsp

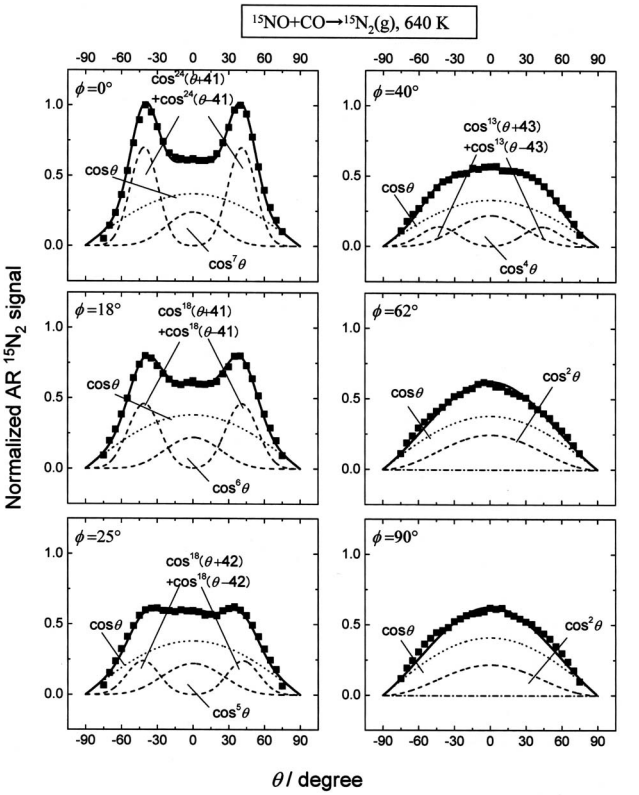

FIG. 5. Angular distributions of desorbing N_2 at different crystal azimuths (ϕ=0°, 18°, 25°, 40°, 62°, and 90°) in the steady-state NO reduction at $P_{NO}=5\times10^{-6}$ Torr, $P_{CO}=2\times10^{-5}$ Torr, and T_S=640 K. The signal is normalized to the maximum value at the collimation angle. Typical deconvolutions are shown by broken and dotted curves. The solid curve indicates the sum of the components. The normally directed N_2 desorption component shows a remarkable anisotropy. Its distribution toward the [001] direction is sharper than that perpendicular to it.

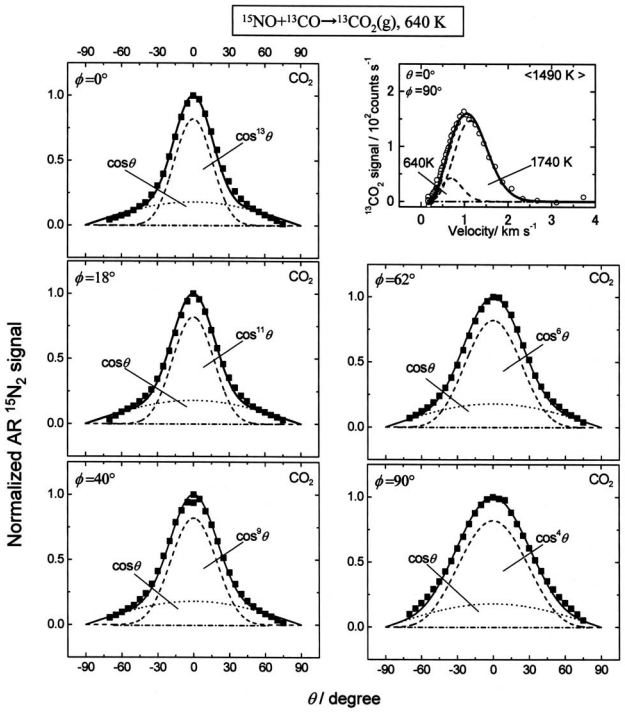

FIG. 6. Angular distributions of desorbing CO_2 at different crystal azimuths (ϕ=0°, 18°, 40°, 62°, and 90°) in the steady-state NO reduction at $P_{NO}=5\times10^{-6}$ Torr, $P_{CO}=2\times10^{-5}$ Torr, and T_S=640 K. The signal is normalized to the value at the surface normal direction. Typical deconvolutions are shown by broken and dotted curves. The solid curve indicates the sum of the components. A typical velocity distribution of desorbing CO_2 in the normal direction is shown in the top-right panel. The deconvoluted velocity distributions are drawn by broken curves.

in the NO+CO reaction under the same condition as that in Fig. 3 are summarized in Fig. 6. The distribution at ϕ=0° is approximated by a $\{0.8\cos^{13}(\theta)+0.2\cos(\theta)\}$ form on the basis of the velocity analysis. At ϕ=90°, it shows a somewhat broader $\{0.8\cos^{4}(\theta)+0.2\cos(\theta)\}$ form. The normally directed component becomes broad with increasing azimuth from the [001] direction. This anisotropy was very close to that in the $CO+O_2$ reaction done on Pd(110).[37]

C. Velocity distribution

The extent of the thermalized component has been estimated from the fraction of the Maxwellian distribution with a translational temperature equal to the surface temperature in the velocity distribution curve. This estimation becomes important for the NO+CO reaction above 600 K where both the normally directed and thermalized components are enhanced. These components have been separated at the normal direction where the contribution from the inclined component is negligible. The translational energy can be used to judge the collimation angle of desorption components because it is peaked at this angle in the repulsive desorption.[4,38]

Each velocity distribution of desorbing N_2 clearly shows the thermalized component in the NO+CO reaction above 550 K. Typical velocity distributions at T_S=550 K and $P_{NO}=P_{CO}=5\times10^{-6}$ Torr are shown in Fig. 7. The resultant mean kinetic energy is shown in the temperature units as $T_{\langle E\rangle}=\langle E\rangle/2k$, where $\langle E\rangle$ is the mean kinetic energy and k is the Boltzmann constant. In the previous paper reporting the desorption angle dependence in the plane along the [001] direction,[21] this value peaked at around ϕ=0° and ϕ=40°, reaching about 3400 K. This time, the crystal-azimuth was varied at a fixed desorption angle of 40°. The translational temperature decreases quickly with increasing azimuth, showing that the desorption is fairly concentrated in the plane along the [001] direction [Fig. 7(e)]. Each velocity distribution curve was too wide to be fitted to one modified Maxwellian form. Especially, the distribution at around θ=40° and $\phi<18°$ is wide, extending to 4 km s^{-1} [Figs. 7(b) and 7(c)].

It should be noted that the distribution curve in the normal direction (θ=0°) involves the component expected by the Maxwellian distribution at the surface temperature, supporting the presence of the cosine component. This component can also be seen at the crystal azimuth above ϕ=40°, where the inclined desorption component is mostly suppressed. The contribution from this cosine component becomes relatively small at around the collimation angle of the inclined component. The translational temperature of desorbing N_2 after subtraction of the thermalized component has been estimated as shown in the figure as the fast component.

This value is peaked at 3420 K at the collimation angle and decreases slowly with increasing shift from the collimated position. It is still 2280 K in the surface normal direc-

Downloaded 16 Apr 2006 to 133.87.245.210. Redistribution subject to AIP license or copyright, see http://jcp.aip.org/jcp/copyright.jsp

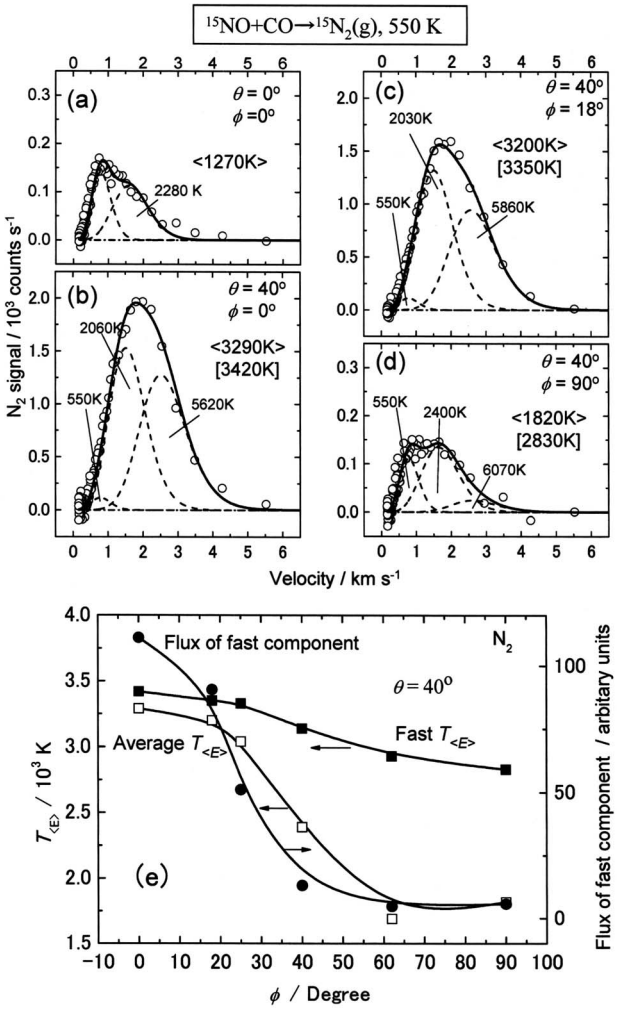

FIG. 7. [(a)–(d)] Velocity distributions of desorbing N_2 in the steady-state NO reduction at a low surface temperature (550 K) and different directions. $P_{NO}=P_{CO}=5\times10^{-6}$ Torr. Typical deconvolutions are shown by broken curves. The solid curve indicates the sum of the components. The N_2 is mostly supplied from the intermediate N_2O decomposition at this temperature. The average kinetic energy is shown in $\langle\ \rangle$ in temperature units and the kinetic energy after subtraction of the thermalized component is in [ ]. (e) The crystal azimuth dependence of the kinetic energy (in temperature units) of desorbing N_2 and its flux at $\theta=40°$ under the above condition. Average $T_{\langle E\rangle}$ (open squares): the average kinetic energy. Fast $T_{\langle E\rangle}$ (closed squares): the average kinetic energy after subtraction of the thermalized component. Its flux (closed circles) is also plotted as fast component. The arrows indicate the corresponding ordinates.

tion and about 2800 K at $\phi=90°$ and $\theta=40°$, where the inclined N_2 desorption does not contribute. The remaining fast component in the normal direction is due to the associative desorption of nitrogen adatoms.[9,12] The presence of normally directed associative desorption of N(a) above about 600 K was already confirmed by Ikai and Tanaka in the isotope labeled experiments described in the Introduction,[10] i.e., the normally directed desorption component above 600 K highly involved $^{15}N_2$ when a Pd(110) surface covered by ^{15}N(a) and ^{14}NO(a) was heated whereas the inclined component consisted of only $^{14}N^{15}N$. The origin of the other fast component observed at $\phi=90°$ and $\theta=40°$ is not clear because of their very small intensity. Two possible causes are considered. First, the normally directed component may be strongly anisotropic, i.e., a broader distribution in the plane along the $[1\bar{1}0]$ direction. Second, a small fraction of the intermediate N_2O may be decomposed when it is oriented along the $[1\bar{1}0]$ direction. The former is likely to take place because of no such component in the N_2O+CO reaction. In fact, the DFT calculations predict that the $[1\bar{1}0]$ oriented N_2O is about 19 kJ mol^{-1} less stable than the [001] oriented species.[28]

The velocity distribution is still wide even after the subtraction of the thermalized component, yielding 1.05–1.10 for the speed ratio defined as $(\langle v^2\rangle/\langle v\rangle^2-1)^{1/2}/(32/9\pi-1)^{1/2}$, where v is the velocity of the molecule, $\langle v\rangle$ is the mean velocity, and $\langle v^2\rangle$ is the mean square velocity. The speed ratio is usually below unity for a hyperthermal component at around the collimation position.[38] A translational temperature of 3420 K corresponds to an energy of 0.59 eV, which is higher than the excitation energy of the molecular vibration of N_2 at the ground state, 0.28 eV.[39] Desorbing fast N_2 may involve vibrationally and/or rotationally excited molecules. In other words, no suitable distribution functions can be invoked for the involved components. Experiments with higher-energy resolutions are highly desired. In order to show the presence of very fast components, the distribution curve has been deconvoluted into two components of the modified Maxwellian distribution, $f(v)=v^3\exp\{-(v-v_0)^2/\alpha^2\}$, where v_0 is the stream velocity and α is the width parameter. Here, we have simply assumed a common width parameter to both components for the deconvolution procedures.[21] The resultant deconvolutions are shown by broken curves. The faster component (in the fast one) is 5600–6100 K wide and the slower one, 2000–2400 K (Fig. 7).

The contributions of both the thermalized and normally directed desorption components are enhanced at higher temperatures and smaller P_{NO}/P_{CO} ratios. The results at 640 K are shown in Fig. 8. The velocity distribution in the normal direction involves a large fraction of the thermalized component [Fig. 8(a)]. This component is significant even at around the inclined collimation angle [Figs. 8(b) and 8(c)]. The translational temperature estimated from the average kinetic energy is lower than that at 550 K although it is peaked at the collimation position, indicating the enhanced contribution from the thermalized component. In fact, the translational temperatures for the fast component obtained after subtraction of the thermalized component are comparable to those obtained at 550 K [Fig. 8(e)]. The velocity curve in the normal direction exhibits the fast component except for the inclined desorption. It should be again noted that the fast component is still significant at $\phi=90°$ and $\theta=40°$ [Fig. 8(d)]. The decay of the fast component flux is less than that at 550 K [Fig. 7(e)] when the azimuth angle shifts from $\phi=0°$ to $\phi=90°$ at $\theta=40°$. We examine the N_2 desorption in the plane along the $[1\bar{1}0]$ direction where no inclined N_2 desorption is contributed from the N_2O decomposition (Fig. 9). The average kinetic energy is not high and insensitive to the desorption angle, consistent with the large fraction of the thermalized component. The kinetic energy of the fast component decreases slowly with increasing desorption angle θ. The flux of the fast component follows roughly a $\cos^2(\theta)$ form.

Downloaded 16 Apr 2006 to 133.87.245.210. Redistribution subject to AIP license or copyright, see http://jcp.aip.org/jcp/copyright.jsp

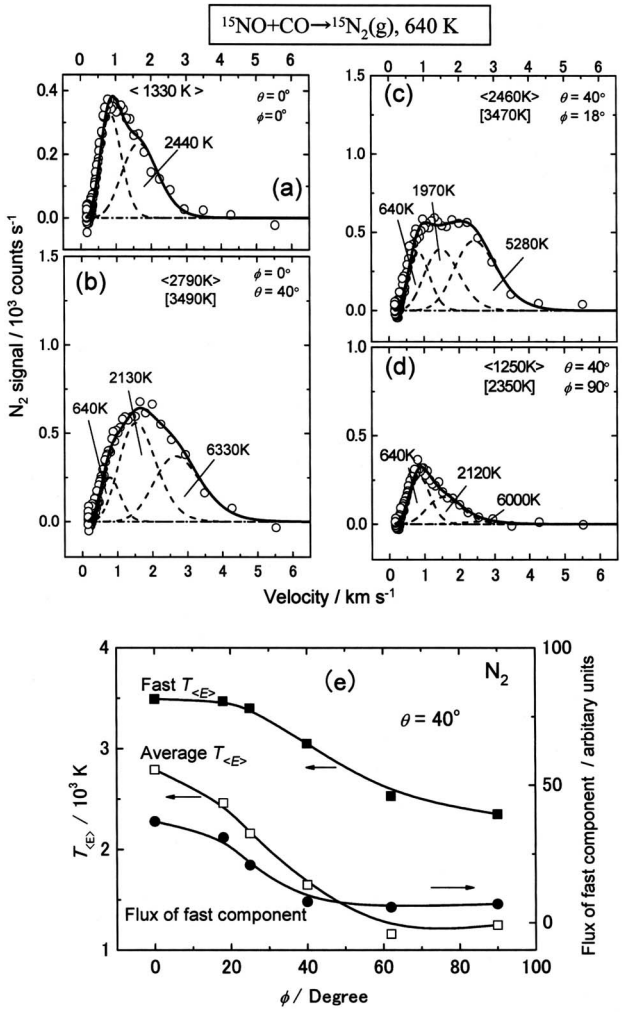

FIG. 8. (a–e) The same as Fig. 7 except that the surface temperature was T_S=640 K, $P_{NO}=5\times10^{-6}$ Torr, and $P_{CO}=2\times10^{-5}$ Torr. However note that the N_2 is largely supplied from the associative process of N(a) at this temperature.

The translational temperature of CO_2 is 1490 K at the normal direction at 640 K (Fig. 6, top-right panel). The velocity distribution contains the thermal component represented by the Maxwellian distribution at the surface temperature. This thermalized CO_2 component was estimated to be about 20% of the total signal at the normal direction. The fast component after subtraction of the thermalized one gives a translational temperature of 1740 K. This component is sharply collimated along the surface normal and becomes very weak at around 45°. The velocity distribution curve at θ=45° off the surface normal involves mostly the thermalized component. The contribution of this component was already studied in the CO oxidation in which it was enhanced under reducing conditions, i.e., when the surface was deficient in O(a). It was explained by the site shift that CO_2 was formed on structural defects suitable for O_2 dissociation.[40] In fact, the product CO_2 formed on defects shows a cosine distribution on stepped platinum surfaces and the energy transfer to the defect was proposed to be quick.[41]

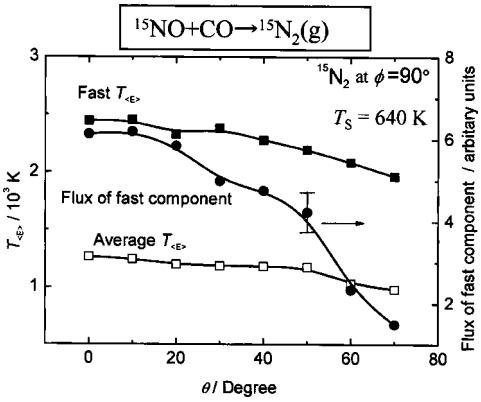

FIG. 9. Flux intensity and translational temperature of desorbing N_2 with desorption angles in the plane along the $[1\bar{1}0]$ direction (ϕ=90°). $P_{NO}=5\times10^{-6}$ Torr, $P_{CO}=2\times10^{-5}$ Torr, and 640 K. Average $T_{\langle E\rangle}$ (open squares): the average kinetic energy. Fast $T_{\langle E\rangle}$ (closed squares): the kinetic energy after subtraction of the thermalized component. Its flux (closed circle) is also plotted as fast component. It should be noted that the flux of the fast component decreases slowly as approximated by a $\cos^2(\theta)$ form, consistent with a slow decay of the kinetic energy.

IV. DISCUSSION

A. Three-dimensional distribution

The CO_2 desorption that is collimated along the surface normal shows remarkable anisotropy. The angular distribution was approximated in a $(0.8\cos^4\theta+0.2\cos\theta)$ form at ϕ=90° and a $(0.8\cos^{13}\theta+0.2\cos\theta)$ form at ϕ=0° in the NO+CO reaction at 640 K (Fig. 6). The angular distribution of the fast component broadens from a $\cos^{13}(\theta)$ form at ϕ=0° to a $\cos^4(\theta)$ form at ϕ=90°. A very similar distribution has been also observed for the CO_2 product in the N_2O+CO reaction and is found to be insensitive to the surface temperature. This anisotropy is also similar to that in the CO oxidation.[37]

It is interesting to examine the extent of anisotropy of the normally directed N_2 desorption. The deconvolution into the three components could be well performed for the data at 640 K as shown in Fig. 5. The signal intensity at around the normal direction is mostly contributed from the normally directed and cosine components. Their relative intensity was well determined from the velocity distribution analysis at the surface normal direction. On the other hand, the signal at around the collimation angle of 41° is merely contributed from the inclined and cosine components. The resultant normally directed component shows an anisotropy, represented by a $\cos^{7\pm2}(\theta)$ form at ϕ=0° and shifts to a $\cos^2(\theta)$ form at ϕ=90°. The distribution is sharper along the [001] direction in a similar way to that of CO_2.

For the anisotropy analysis of the inclined N_2 desorption, the following transformation from the polar coordinates to another polar angle system was necessary. The desorption direction can be defined with two new angles α and β [see Fig. 1(c)]. According to the rotation defining Eulerian angles, the relation between angles (α,β) and (θ,ϕ) is given by $\cos\theta=\cos\alpha\cos\beta$ and $\tan\phi=-\tan\beta/\sin\alpha$.[42] α is the longitude measured from the normal direction [110] about the $[\bar{1}10]$ axis when the polar axis is taken to be parallel to the

Downloaded 16 Apr 2006 to 133.87.245.210. Redistribution subject to AIP license or copyright, see http://jcp.aip.org/jcp/copyright.jsp

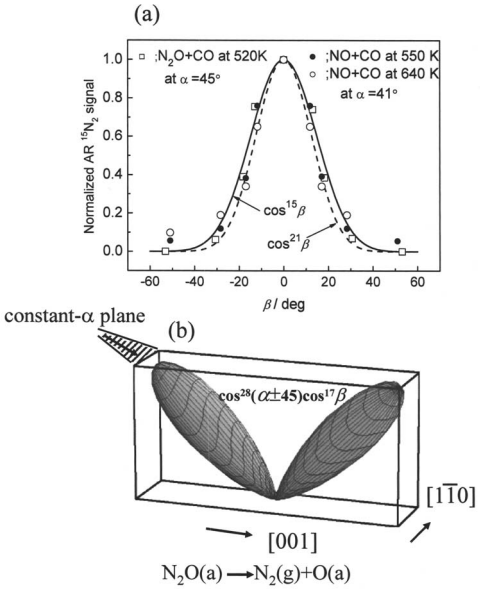

FIG. 10. (a) N_2 angular distributions (β dependence) in the inclined plane at $\alpha=45°$ for the N_2O+CO reaction and at $\alpha=41°$ for the NO+CO reaction. (b) N_2 distribution in the N_2O+CO reaction in three-dimensional coordinates at 550 K.

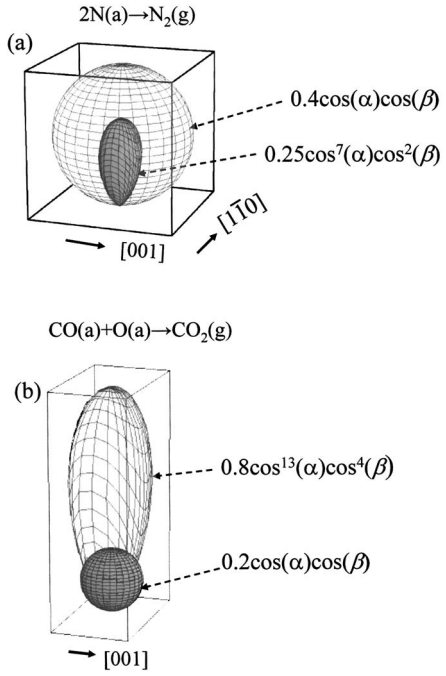

FIG. 11. Spatial distributions in three-dimensional coordinates of desorbing (a) N_2 in the $2N(a)\rightarrow N_2(g)$ process and (b) CO_2 in the NO+CO reaction at 640 K.

crystal azimuth [$\bar{1}$10], whereas β becomes the longitude shifted from the plane along the [001] direction when the polar axis is parallel to the [001] axis. When $\beta=0°$, the value of α becomes equal to the desorption angle (θ) in the plane along the [001] direction. The experimental AR signals at definite (θ,ϕ) values were converted into the signal intensity at new coordinates (α,β) after smoothing the data points against varying θ values at fixed ϕ values. The resultant correction due to the smoothing procedures, however, was less than 10% of each signal because of the measurement at every 5° of the θ value. The signals estimated at $\alpha=45°$ for the N_2O+CO reaction are shown as a function of β in Fig. 10(a). The β value is always less than ϕ at a fixed α value, and then the distribution at a fixed α value against β becomes sharper than that against ϕ. The resultant distribution at $\alpha=45°$ has been approximated by a $\cos^n\beta$ form with $n=17\pm3$. Very similar β dependences have been obtained at $\alpha=41°$ from the inclined N_2 desorption in the NO+CO reaction at 550 and 640 K.

The spatial distributions of desorbing N_2 and CO_2 are shown in three-dimensional polar coordinates in Figs. 10(b) and 11, which were derived from the angular distribution data in Figs. 4–6. These were drawn by assuming a distribution with twofold symmetry around the collimation axis at $\theta=45°$ and $\phi=90°$ for the inclined N_2, and at $\theta=0°$ for CO_2 and the normally directed N_2 desorption component. The distribution below 550 K for desorbing N_2 mostly consists of a single desorption component that is merely controlled by the N_2O decomposition. In this new three-dimensional way, the N_2 distribution for the N_2O+CO reaction is approximated by $\cos^{28}(\alpha\pm45)\cos^{17}(\beta)$. The N_2 distribution for the NO+CO reaction has the form of $\cos^{22}(\alpha\pm41)\cos^{17}(\beta)$ at 550 K. This distribution form describes almost all the signal intensity of the fast component.

Similarly, the fast CO_2 component is approximated as a $\cos^{13}\alpha\cos^4\beta$ form, commonly for the N_2O+CO and NO+CO reactions. This anisotropy is very close to that in the $CO+O_2$ reaction on Pd(110).[37] The normally directed N_2 desorption is approximated by a $\cos^7\alpha\cos^2\beta$ form. The distribution is commonly sharper in the plane along the [001] direction.

B. Intermediate structure

A Pd(110) plane shows a stable (1×1) form, whereas it is reconstructed into missing-row forms when it is covered by oxygen.[43–45] The resultant surface consists of three- or four-atom-wide microfacets with a (111) structure declining alternatively about +30° or −30° in the [001] direction.[46] The repulsive force exerting from its formation site to the product CO_2 in CO oxidation on noble metals is strong enough to hold the site orientation in the angular distributions.[4] In fact, the reactive CO_2 desorption in AR-TPD as well as steady-state (SS) CO oxidation experiments collimates fairly along the local normal of declining microfacets on reconstructed Pt(110), Ir(110), and Rh(110), indicating the CO_2 formation on inclined (111) facets.[4] On the other hand, no inclined CO_2 desorption has been found on Pd(110) under either TPD or SS conditions, although the $c(2\times4)$-O lattice due to the missing-row structure was observed.[37,40] The lack of inclined CO_2 desorption on this surface is due to either the instability of the (1×2) reconstruction without oxygen above 355 K,[47] or high oxygen coverage. The CO_2 desorption shifts to the surface normal direction when the (1×2) surface is highly covered by oxygen.[47,48] The observation of inclined CO_2 desorption requires low-oxygen coverage conditions. However, the reconstructed Pd(110)(1×2) stabilized by oxygen is

Downloaded 16 Apr 2006 to 133.87.245.210. Redistribution subject to AIP license or copyright, see http://jcp.aip.org/jcp/copyright.jsp

converted into the (1×1) form when the surface oxygen is removed above 355 K.[43] The (1×2) reconstruction by CO appears only at high CO coverage.[49–52]

LEED observations were consistent with the absence of bidirectional CO_2 desorption in N_2O or NO reduction. The LEED pattern due to c(2×4)-O or (2×3)-1D-O was suppressed with increasing CO pressures, yielding more products. The rate-determining NO or N_2O dissociation proceeds on (1×1) parts without oxygen. The CO_2 formation takes place on the oxygen-covered area where the oxygen density is high enough to emit CO_2 along the surface normal.

On the other hand, the inclined N_2 desorption takes place on (1×1) parts because of the severe retardation by oxygen toward N_2O dissociation.[17,53] The intermediate N_2O is easily formed from the reaction N(a)+NO(a) in NO reduction on palladium, platinum, and rhodium surfaces.[12,23–25] The reaction pathway through N_2O decomposition is operative at low temperatures where NO(a) is significant, more than N(a).[54] N_2O is easily decomposed on Pd(110) below 150 K, emitting N_2 in the inclined way.[15–18] This peculiar desorption has been proposed to be due to the decomposition of N_2O oriented along the [001] direction although the vibrational spectroscopy work indicates the terminal nitrogen atom interacting with the surface at around 100 K,[55] or no N_2O(a) signal has been observed in the catalyzed NO reduction above 500 K.[56–58] On clean Pd(110), DFT-GGA,[27,28] STM,[29] and NEXAFS[30] studies commonly support the presence of two adsorption forms below 60 K, i.e., one lying form oriented along the [001] direction and another tilted form with the terminal nitrogen atom interacting with the metal. This is consistent with the results from vibrational spectroscopy which is insensitive to the lying form according to the surface-selection rule.[59] The activation energy barrier between the tilted and lying forms has been estimated to be only 4 kJ mol^{-1} by DFT-GGA and 8 kJ mol^{-1} in the reverse way, i.e., the conversion between them seemed to be facile.[28] The lying N_2O oriented along the [001] direction bridges the palladium-atom trough running along the $[1\bar{1}0]$ direction and is located on the on-top site.

C. Different collimation angles

The above collimation angle of desorbing N_2 shows noticeable differences between NO and N_2O reduction, i.e., $41\pm2°$ and $45\pm2°$, respectively. It is not likely that the intermediate N_2O in the NO reduction is in different adsorption states from those of N_2O(a) supplied from gaseous N_2O as proposed by Ikai and Tanaka,[10] because some fraction of the intermediate desorbs without dissociation after thermalization as observed in its cosine distribution. Rather, the intermediate N_2O may be affected by coadsorbed species, such as NO(a) and/or N(a) which are absent in the N_2O+CO reaction.

In fact, the collimation angle of desorbing N_2 from N_2O decomposition has been reported to be affected by coadsorbed species and the kind of metal. In AR-TPD work on adsorbed N_2O on Pd(110), the collimation angle of desorbing N_2 shifts at low N_2O density.[17] There are four N_2 desorption peaks in the range of 100–160 K, i.e., β_4-N_2 peaked at 110 K at very low N_2O(a) density, collimated at 50°, and shifted to 44° with increasing N_2O coverage. The β_3-N_2 peak at 123 K and β_1-N_2 at around 150 K appearing at higher N_2O density are collimated at $44\pm2°$. The N_2O density above 470 K is very low because of the small heat of adsorption, about 37 kJ mol^{-1}. Thus, the intermediate N_2O is decomposed in a situation similar to β_4-N_2, which suggests that the collimation angle of N_2 emission is affected by the coadsorbed species in the steady-state NO reduction rather than N_2O reaction.

The Pd(110) surface is covered by CO(a) or O(a) in the course of N_2O reduction. The collimation angle of N_2 desorption remains invariant even when the reaction shifts from the active region into the inhibited region, i.e., the main surface species changes from O(a) to CO(a) although the amount of O(a) is very small. Thus, the effect to the collimation from CO(a) is minor or nonexistent, since the CO coverage increases by as much as 0.2 monolayer at the kinetic transition.[60] This is close to the coverage of the p(2×2)-CO lattice.[49,50] The coverage of O(a) and N(a) may increase to much higher levels in the active region of the NO reduction than that in the N_2O reaction because the sticking probability of NO is much larger than that of N_2O.[54] In fact, adsorbed oxygen atoms play a role of not only an inhibitor toward N_2O dissociation but also a stabilizer of it. In the presence of adsorbed oxygen, the heat of N_2O adsorption increases from around 30 to 43 kJ $mole^{-1}$ on Ru(0001).[61] However, no collimation angle shift has been observed on Rh(110) as a result of the addition of O(a) although the TPD decomposition peak shifted from 70 to 140 K.[13,19] Rather, the intermediate N_2O may be affected by coadsorbed species, such as N(a) and NO(a). The coverage of N(a) may also be significant in the NO reduction.[54] The N(a)-covered palladium was reported to be active toward N_2 adsorption even at room temperature,[62] probably toward N_2O as well.

The collimation angle of the product N_2 depends on metal, i.e., $70°\pm5°$ on Rh(110), $65°\pm5°$ on Ir(110), and 43°–50° on Pd(110). This sequence is consistent with the hot atom-assisted desorption model. In this model, a nascent oxygen atom (hot atom) provides a surface-parallel momentum to desorbing N_2 when N_2O(a) molecules oriented along the [001] direction are decomposed. This hot atom-assisted model predicts larger collimation angles and higher kinetic energy on rhodium and iridium than on palladium because larger amounts of energy are released in the metal-O bond formation.[63] During stabilization of the nascent product O(a) in N_2O dissociation, a large amount of the energy due to the O-metal bonding must be dissipated; the available energy that can be delivered to the product comes primarily from the metal-O bond formation.[63,64] The released energy may be reduced when the N_2O dissociation site is affected by either N(a) or O(a). The decreased amount of released energy may provide less momentum transfers toward desorbing N_2 and then yield smaller collimation angles.

D. Anisotropy in desorption

The anisotropy of the spatial distribution of desorbing products has been due to either the anisotropic structures of

Downloaded 16 Apr 2006 to 133.87.245.210. Redistribution subject to AIP license or copyright, see http://jcp.aip.org/jcp/copyright.jsp

the product formation site or the anisotropic movements of the parent molecules. The former was proposed for anisotropic CO_2 distributions in the CO oxidation on Pd(110), Pt(110)(1×2), Ir(110)(1×2), and other stepped platinum surfaces.[4] The movement at the transition state (TS) is restricted by the potential-energy field of the atoms involved and particularly, strongly depends on the structural anisotropy of the reaction site. The distribution is sharp when the movement is restricted, while facile movements will yield a broader angular distribution.[4,65] This model originated from the theoretical treatment of the *associative desorption* dynamics of adsorbed hydrogen atoms.[66,67] In the other case, anisotropy in *dissociative desorption* is explained to be due to the motion of the parent molecule. This model has been frequently used in ESDIAD.[7,8] For example, this is the case of excited CO desorption in ESDIAD on a stepped Pt(112) surface, in which the angular distribution becomes broader in the plane where the molecule is easily vibrated (i.e., the restricted vibration immediately before bond breaking).[68] These two models are applicable for the present N_2 desorption in the different pathways.

The sharpness of the angular distribution of desorbing molecules is related to the extent of repulsive forces operative toward the molecules.[4] The stronger is the repulsive force the higher is the velocity and the sharper is the distribution of desorbing molecules. The sharpness is reduced by the TS motions perpendicular to the rupturing bond axis, typically, the thermal motions of TS or the parent molecules.[68] This latter factor induces anisotropy in the product distribution. In the normally directed N_2 desorption, the product is formed in an associative process of adsorbed nitrogen atoms and the resultant bulky N_2 molecule is repulsed from the formation site, being emitted along the local normal of the site. Anisotropic motions of the nascent bulky N_2 molecule may be expected. On Pd(110), the motion along the $[1\bar{1}0]$ direction is facile since the palladium atoms are closely packed allowing the molecule to move easily. On the other hand, the movement along the [001] direction may be restricted because of the high atomic corrugation. In fact, nitrogen adatoms are proposed to be located on the long-bridge site in the trough from high-resolution electron energy-loss spectroscopy (HREELS) work.[69] The transition state of N_2 being desorbed may be moved along the $[1\bar{1}0]$ direction more easily than that along the [001] direction.

The inclined N_2 emission requires another anisotropy mechanism available to dissociative desorption since N_2 is directly emitted in the N_2O dissociation event. The angular distribution of desorbing N_2 in the inclined way is sharper in the plane along the [001] direction than that perpendicular to it. The sharpness parameter of the distribution is $n=28$ at $T_S=400$ K, where the distribution is represented in a $\cos^n(\delta)$ form. δ is the angle shift from the collimation position. The parameter increases to $n=50$ at $T_S=110$ K in the AR-TPD work[17] and decreases to $n=18$ at 750 K. On the other hand, the parameter in the inclined plane passing $\alpha=45°$, was estimated to be $n=17\pm3$ at 550 K. The movement of the N_2O molecule is more restricted in the plane along the [001] direction. This is consistent with the results from DFT-GGA, which predict that the dissociation is much easier from the bridge site although the [001] oriented N_2O is more stable over the on-top sites.[28] The potential-energy surface around the bridge site shows an extremely shallow local minimum, hence the movement around the bridge site would be very facile toward the $[1\bar{1}0]$ direction.

In ESDIAD, the orientation of the parent molecule immediately before dissociation is clear since the reactant is in a stable adsorption state and the (electronic) transition from it to the dissociative form is faster than the nuclear motions. At present, a reliable model to predict the inclined N_2 collimation angle is not available. Indeed, even the dissociation sequence of N_2O is not clear, i.e., the DFT work predicts that the N–O bond is first broken in $N_2O(a)$ because the adsorption through the terminal oxygen is not predicted on clean Pd(110).[64] On the other hand, the first scission may take place in the N-metal bond when that adsorption is possible. This adsorption form has been proposed on several oxides. The restricted vibration of N_2O obliquely standing through the terminal oxygen is suitable for anisotropic desorption as expected in the ESDIAD model. There must be a limited angle range suitable for the NN–O bond scission on oxygen-modified Pd(110).

V. CONCLUSIONS

The product desorption in the steady-state NO+CO and N_2O+CO reactions on Pd(110) has been studied by using angle-resolved flux and velocity distribution measurements and LEED observations. The following results have been obtained:

(1) N_2 desorption in both reactions splits into two directional lobes collimated along 41°–45° from the surface normal toward the [001] and $[00\bar{1}]$ directions. This N_2 is emitted in the decomposition of the intermediate N_2O oriented along the [001] direction.
(2) Above 550 K, the normally directed N_2 desorption is enhanced in the NO reduction. This comes from the associative desorption of N(a).
(3) Reactive CO_2 desorption is collimated sharply along the surface normal in both reactions.
(4) Each product desorption component shows a remarkable asymmetric distribution around their collimation axis. Commonly, the distribution is sharper in the plane along the [001] direction than in that perpendicular to it.

ACKNOWLEDGMENTS

The authors thank A. Hiratsuka for the data analyses and figure drawings. One of the authors (A.K.) acknowledges the support that he received from the Japan Society of the Promotion of Science (JSPS). This work was partly supported by the Joint Studies Program (2005) of the Catalysis Research Center and by the 1996 COE special equipment program of the Ministry of Education, Sports, and Culture of Japan.

Downloaded 16 Apr 2006 to 133.87.245.210. Redistribution subject to AIP license or copyright, see http://jcp.aip.org/jcp/copyright.jsp

[1] W. S. Epling, L. E. Campbell, A. Yezerets, N. W. Currier, and J. E. Parks II, Catal. Rev. - Sci. Eng. **46**, 163 (2004).
[2] T. Matsushima, I. I. Rzeznicka, and Y.-S. Ma, Chem. Rec. **5**, 81 (2005).
[3] N. W. Cant, D. E. Angove, and D. C. Chambers, Appl. Catal., B **17**, 63 (1998).
[4] T. Matsushima, Surf. Sci. Rep. **52**, 1 (2003).
[5] V. P. Zhdanov and B. Kasemo, Surf. Sci. Rep. **29**, 31 (1997).
[6] A. Hodgson, Prog. Surf. Sci. **63**, 1 (2000).
[7] R. H. Stulen, Prog. Surf. Sci. **32**, 1 (1989).
[8] R. D. Ramsier and J. T. Yates, Jr., Surf. Sci. Rep. **12**, 243 (1991).
[9] T. Matsushima, Surf. Sci. **197**, L287 (1988).
[10] M. Ikai and K.-I. Tanaka, J. Phys. Chem. B **103**, 8277 (1999).
[11] J. I. Colonell, K. D. Gibson, and S. J. Sibener, J. Chem. Phys. **104**, 6822 (1996).
[12] M. Ikai and K.-I. Tanaka, Surf. Sci. **357/358**, 781 (1996).
[13] K. Imamura and T. Matsushima, Catal. Lett. **97**, 197 (2004).
[14] K.-I. Tanaka and M. Ikai, Top. Catal. **20**, 25 (2000).
[15] Y. Ohno, K. Kimura, M. Bi, and T. Matsushima, J. Chem. Phys. **110**, 8221 (1999).
[16] Y. Ohno, I. Kobal, H. Horino, I. I. Rzeznicka, and T. Matsushima, Appl. Surf. Sci. **169/170**, 273 (2001).
[17] H. Horino, S. Liu, A. Hiratsuka, Y. Ohno, and T. Matsushima, Chem. Phys. Lett. **341**, 419 (2001).
[18] H. Horino, I. I. Rzeznicka, A. Kokalj, I. Kobal, A. Hiratsuka, Y. Ohno, and T. Matsushima, J. Vac. Sci. Technol. A **20**, 1592 (2002).
[19] K. Imamura, H. Horino, I. I. Rzeznicka, A. Kokalj, I. Kobal, A. Hiratsuka, B. E. Nieuwenhuys, and T. Matsushima, Surf. Sci. **566/568**, 1076 (2004).
[20] Y.-S. Ma, I. I. Rzeznicka, and T. Matsushima, Chem. Phys. Lett. **388**, 201 (2004).
[21] I. I. Rzeznicka, Y.-S. Ma, G. Cao, and T. Matsushima, J. Phys. Chem. B **108**, 14232 (2004).
[22] Y.-S. Ma and T. Matsushima, J. Phys. Chem. B **109**, 1256 (2005).
[23] H. Wang, R. G. Tobin, C. L. DiMaggio, G. B. Fisher, and D. K. Lambert, J. Chem. Phys. **107**, 9569 (1997).
[24] D. N. Belton, C. L. DiMaggio, S. J. Schmieg, and K. Y. Simon Ng, J. Catal. **157**, 559 (1995).
[25] R. G. Sharpe and M. Bowker, Surf. Sci. **360**, 21 (1996).
[26] E. J. Heiweil, M. P. Casassa, R. R. Cavanagh, and J. T. Stephensen, Annu. Rev. Phys. Chem. **40**, 143 (1989).
[27] A. Kokalj, H. Horino, Y. Ohno, I. Kobal, and T. Matsushima, Surf. Sci. **506**, 196 (2002).
[28] A. Kokalj, I. Kobal, and T. Matsushima, J. Phys. Chem. B **107**, 2741 (2003).
[29] K. Watanabe, A. Kokalj, Y. Inokuchi, I. I. Rzeznicka, K. Ohshimo, N. Nishi, and T. Matsushima, Chem. Phys. Lett. **406**, 474 (2005).
[30] K. Watanabe, A. Kokalj, H. Horino, I. I. Rzeznicka, T. Takahashi, N. Nishi, and T. Matsushima Jpn. J. Appl. Phys. **45** (3B), 2290 (2006).
[31] H. H. Sawin and R. P. Merrill, J. Chem. Phys. **73**, 996 (1980).
[32] M. Kobayashi and Y. Tuzi, J. Vac. Sci. Technol. **16**, 685 (1979).
[33] G. Comsa, R. David, and B. J. Schumacher, Rev. Sci. Instrum. **52**, 789 (1981).
[34] D. N. Belton, C. L. DiMaggio, and K. Y. Simon Ng, J. Catal. **144**, 273 (1993).
[35] J. W. He, U. Memmert, and P. R. Norton, J. Chem. Phys. **90**, 5082 (1989).
[36] Y.-S. Ma, A. Kokalj, and T. Matsushima, Phys. Chem. Chem. Phys. **7**, 3716 (2005).
[37] T. Matsushima, K. Shobatake, Y. Ohno, and K. Tabayashi, J. Chem. Phys. **97**, 2783 (1992).
[38] G. Comsa and R. David, Surf. Sci. Rep. **5**, 145 (1985).
[39] A. A. Radzig and B. M. Smirnov, *Reference Data on Atoms, Molecules and Ions* (Springer, Berlin, 1985).
[40] Md. G. Moula, S. Wako, G. Cao, K. Kimura, Y. Ohno, I. Kobal, and T. Matsushima, Phys. Chem. Chem. Phys. **1**, 3677 (1999).
[41] J. Segner, C. T. Campbell, G. Doyen, and G. Ertl, Surf. Sci. **138**, 505 (1984).
[42] H. Goldstein, *Classical Mechanics*, 2nd ed. (Addison-Wesley, Reading, 1980) p. 143.
[43] V. R. Dhank, G. Comelli, G. Paolucci, K. C. Prince, and R. Rosei, Surf. Sci. **260**, L24 (1992).
[44] H. Tanaka, J. Yoshinobu, and M. Kawai, Surf. Sci. **327**, L505 (1995).
[45] R. A. Bemmett, S. Poulstone, I. Z. Jones, and M. Bowker, Surf. Sci. **401**, 72 (1998).
[46] E. C. Sowa, M. A. van Hove, and D. L. Adams, Surf. Sci. **199**, 174 (1988).
[47] I. I. Rzeznicka and T. Mataushima, Chem. Phys. Lett. **377**, 279 (2003).
[48] Md. G. Moula, A. B. P. Mishra, I. Rzeznicka, M. U. Kislyuk, S. Liu, Y. Ohno, and T. Matsushima, Chem. Phys. Lett. **341**, 225 (2001).
[49] R. Raval, S. Haq, M. A. Harrison, G. Blyholde, and D. A. King, Chem. Phys. Lett. **167**, 391 (1990).
[50] R. Raval, S. Haq, G. Blyholder, and D. A. King, J. Electron Spectrosc. Relat. Phenom. **54/55**, 629 (1990).
[51] P. Hu, L. Morales de la Garza, R. Raval, and D. A. King, Surf. Sci. **249**, 1 (1991).
[52] A. Gaussmann and N. Kruse, Surf. Sci. **279**, 319 (1992).
[53] S. Liu, H. Horino, A. Kokalj, I. I. Rzeznicka, K. Imamura, Y.-S. Ma, I. Kobal, Y. Ohno, A. Hiratsuka, and T. Matsushima, J. Phys. Chem. B **108**, 3828 (2004).
[54] M. Bowker, R. A. Bennett, and I. Z. Jones, Top. Catal. **28**, 25 (2004).
[55] S. Haq and A. Hodgson, Surf. Sci. **463**, 1 (2000).
[56] Y. Izumi, T. Kizaki, and K.-I. Aika, Bull. Chem. Soc. Jpn. **74**, 1499 (2001).
[57] E. Ozensoy, C. Hess, and D. W. Goodman, J. Am. Chem. Soc. **124**, 8524 (2002).
[58] E. Ozensoy and D. W. Goodman, Phys. Chem. Chem. Phys. **6**, 3765 (2004).
[59] N. V. Richardson and N. Sheppard, in *Vibrational Spectroscopy of Molecules on Surfaces*, edited by J. T. Yates, Jr. and T. E. Madey (Plenum, New York, 1987) p. 1.
[60] Y.-S. Ma, S. Han, and T. Matsushima, Langmuir **21**, 9529 (2005).
[61] H. H. Huang, C. S. Seet, Z. Zou, and G. Q. Xu, Surf. Sci. **356**, 181 (1996).
[62] E. Miyazaki, I. Kojima, and S. Kojima, Langmuir **1**, 264 (1985).
[63] W. A. Brown, R. Kose, and D. A. King, Chem. Rev. (Washington, D.C.) **98**, 797 (1998).
[64] I. Kobal, A. Kokalj, H. Horino, Y. Ohno, and T. Matsushima, Trends Chem. Phys. **10**, 139 (2002).
[65] T. Matsushima, J. Chem. Phys. **91**, 5722 (1989).
[66] Y. Ohno, T. Nakmura, and H. Kita, Appl. Phys. A: Solids Surf. **50**, 551 (1990).
[67] Y. Ohno, T. Nakamura, and H. Kita, Appl. Phys. A: Solids Surf. **51**, 35 (1990).
[68] M. A. Henderson, A. Szabó, and J. T. Yates Jr., Chem. Phys. Lett. **168**, 51 (1990).
[69] Y. Kuwahara, M. Fujisawa, M. Jo, M. Onchi, and M. Nishijima, Surf. Sci. **188**, 490 (1987).

Downloaded 16 Apr 2006 to 133.87.245.210. Redistribution subject to AIP license or copyright, see http://jcp.aip.org/jcp/copyright.jsp